arXiv:1512.00696v1 [quant-ph] 2 Dec 2015

Quantum signature for laser-driven correlated excitation of Rydberg atoms

Huaizhi Wu,[1] Yong Li,[2] Zhen-Biao Yang,[1] and Shi-Biao Zheng[1]
[1] *Department of Physics, Fuzhou University, Fuzhou 350116, People's Republic of China,*
[2] *Beijing Computational Science Research Center, Beijing 100193, People's Republic of China*

The excitation dynamics of a laser-driven Rydberg gas exhibits cooperative effect due to the interatomic Rydberg-Rydberg interaction, but the large many-body system with inhomogeneous Rydberg coupling is hard to be exactly solved or numerically studied by density matrix equations. In this paper, we find that the laser-driven Rydberg gas with most of the atoms being in the ground state can be described by a simplified interaction model resembling the optical Kerr effect if the distance-dependent Rydberg-Rydberg interaction is replaced by an infinite-range coupling. We can then quantitatively study the effect of the quantum fluctuations on the Rydberg excitation with the interatomic correlation involved and analytically calculate the statistical characteristics of the excitation dynamics in the steady state, revealing the quantum signature of the driven-dissipative Rydberg gas. The results obtained here will be of great interest for other spin-1/2 systems with spin-spin coupling.

PACS numbers: 32.80.Ee, 03.65.Yz, 42.50.Ct

Introduction - A laser-driven Rydberg gas in which the Rydberg excited atoms experience the long-ranged dipole-dipole or van der Waals interaction potential can exhibit atomic many-body correlations that are of great interest for future applications in quantum information processing [1] and quantum nonlinear optics [2]. While much attention has been recently devoted to the enhancement of optical nonlinearity by mapping the Rydberg-Rydberg correlation onto optical field [3–13] and to the nonequilibrium quantum phenomena [14–20] and the preparation of Rydberg crystals [21–23] by modulating the driven-dissipative dynamics, the quantitative understanding of the excitation process for the Rydberg gas itself is of particular interest on the other hand and is not yet clear.

There has been a lot of theoretical work focusing on the excitation dynamics in both the coherent [24–31] and dissipative regimes [32–40]. Generally, the system was analyzed via a mean-field treatment disregarding the interatomic correlation [18, 19, 23, 32, 38], a variational approach allowing for an approximation of the true steady state [39] or a perturbation theory up to fourth order [33, 37, 40]. Alternatively, the incoherent dynamics can be numerically simulated on account of strong dissipation via the rate equation [25, 36], and weak decay via the density-matrix master equation [28] (or equivalently the wave-function Monte Carlo approach [33–36, 38]) and the density-matrix renormalization-group [22] that are normally useful for the lattice geometrics consisting of several tens of atoms.

The excitation dynamics under resonant and off-resonant driving exhibits different counting statistics of the Rydberg atom number. While the resonant driving leads to reduced number fluctuations of the Rydberg excitations [30, 41, 42], the off-resonant coupling offers richer physics such as the experimentally observed optical bistability [43], Rydberg aggregates [44, 45], bimodal counting distribution [46], and kinetic constraints [47]. In addition, of special interest for the experimental analysis is the formation mechanism of the collective many-body states since the statistical characteristics [44, 46] and direct imaging [48, 49] are challenging for distinguishing sequential and simultaneous excitation process of the Rydberg atoms. These have also been theoretically studied via the analytical model with generalized Dicke states [41] or Monte Carlo simulation [44].

In this paper, we study the excitation dynamics of a laser driven-dissipative Rydberg gas in the Holstein-Primakoff regime, i.e. the majority of atoms remain in the ground state as is the case in the experiment [44, 46]. To give an intuitive understanding, we make use of a simplified picture for the many-body system as in ref. [34], where the characteristic C_μ/R^μ ($\mu = 3, 6$) dependent interaction for atom pairs with the separation R is replaced by an infinite-range coupling. It allows us to regard the system as a nonlinear optical polarizability model [50] and quantitatively study the effect of quantum correlations on the excitation dynamics in the steady state. We find from the linearized calculation that the quantum fluctuations to the first order will enhance the Rydberg population [34, 37] and modulate the fluctuation of the collective excitation number. Moreover, the pure quantum effects like pair excitation of Rydberg atoms can be clearly revealed by the full quantum results after comparison with the classical steady-state solution. Our finding not only connects to the recent experimental observations for the many-body system with Rydberg-Rydberg coupling, but also relates to the trapped spin-1/2 ions system where the spin-spin couplings are mediated by the motional degrees of freedom [51].

Model - Consider a system of N atoms ($N \gg 1$) that are excited from the ground state $|g_j\rangle$ to a Rydberg state $|e_j\rangle$ by a continuous and spatially uniform laser beam with the detuning Δ from atomic resonance and the Rabi

frequency Ω (assumed to be real). By including the all-to-all interatomic coupling χ, the Hamiltonian in the interaction picture and rotating-wave approximation reads ($\hbar = 1$) [34]

$$H = \sum_{j=1}^{N}\left[-\Delta|e_j\rangle\langle e_j| + \frac{\Omega}{2}(|e_j\rangle\langle g_j| + |g_j\rangle\langle e_j|)\right] + \chi\sum_{j<k}|e_j\rangle\langle e_j|\otimes|e_k\rangle\langle e_k|. \quad (1)$$

We now introduce the collective spin operators $S^+ = \sum_{j=1}^{N}|e_j\rangle\langle g_j|$ and $S^- = \sum_{j=1}^{N}|g_j\rangle\langle e_j|$, which according to the Holstein-Primakoff transformation can be expressed in terms of the bosonic operators b and $b^\dagger$ (with $[b, b^\dagger] = 1$) as $S^+ = b^\dagger\sqrt{N - b^\dagger b}$ and $S^- = \sqrt{N - b^\dagger b}b$ if the lowest energy level of these new operators is set to be the atomic state in which all of the atoms are in the ground state [52, 53]. It follows that $\sum_{j=1}^{N}|e_j\rangle\langle e_j| = \frac{1}{2}[S^+, S^-] + \frac{N}{2} = b^\dagger b$ and $\sum_{j<k}|e_j\rangle\langle e_j|\otimes|e_k\rangle\langle e_k| = \frac{1}{2}b^\dagger b^\dagger bb$. We then focus on the parameter regime as in the recent experiments where the mean number of Rydberg excitations is much less than the total number of atoms (i.e. $\bar{n}_e \equiv \langle b^\dagger b\rangle \ll N$) resulting in $S^+ \simeq \sqrt{N}b^\dagger$, $S^- \simeq \sqrt{N}b$ [44, 46]. Thus, the Hamiltonian of the system can be rewritten by

$$H_b = -\Delta b^\dagger b + \frac{\chi}{2}b^\dagger b^\dagger bb + \lambda(b + b^\dagger) \quad (2)$$

with $\lambda = \sqrt{N}\Omega/2$. Note that the system involving the Rydberg-Rydberg coupling behaves in resemblance to the optical Kerr nonlinearity and its coherent dynamics will remain in the symmetric Dicke state space. However, the spontaneous decay from the Rydberg excited state (with the relaxation rate γ) may lead to incoherent mixture with the asymmetric dark states. For clarity, our work will focus on the state space mainly spanned by null and single Rydberg excitation accompanied by a tiny fraction of double excitations. The Rydberg population is confirmed by direct simulations of the master equation $\dot{\rho} = -i[H_b, \rho] + \frac{\gamma}{2}(2b\rho b^\dagger - \rho b^\dagger b - b^\dagger b\rho)$ for a zero-temperature thermal reservoir, and the counting statistics of Rydberg excitation is quantified by the Mandel Q parameter defined as $Q = \langle(\Delta\hat{n}_e)^2\rangle/\langle\hat{n}_e\rangle - 1$ with $\hat{n}_e \equiv b^\dagger b$, as shown in Fig. 1. The exact simulation of the dissipative dynamics for few atoms with the Hamiltonian Eq. (1) can be found in Ref. [54], which shows good agreement with the bosonization model.

Classical dynamics - The quantum Langevin equation of motion for the bosonic system is

$$\dot{b} = -i\lambda - i\Gamma b - i\chi b^{\dagger 2}b + \xi(t) \quad (3)$$

where $\Gamma = -(\Delta + i\gamma/2)$ might include the decoherence due to the laser linewidths and doppler broadening, and $\xi(t)$ is the zero-value-mean noise operator. Beyond the mean-field theory, here the correlation between atoms is retained in the evolutional dynamics. In the classical limit, the equation of motion for $\bar{\alpha} = \langle b\rangle$ ($\bar{\alpha}^* = \langle b^\dagger\rangle$) are given by

$$\dot{\bar{\alpha}} = -i\lambda - i\bar{\alpha}(\Gamma + \chi|\bar{\alpha}|^2),$$

$$\dot{\bar{\alpha}}^* = i\lambda + i\bar{\alpha}^*(\Gamma^* + \chi|\bar{\alpha}|^2). \quad (4)$$

Then, the mean number of Rydberg excitations $\bar{n}_{es} = |\bar{\alpha}_s|^2$ in the steady state fulfills the algebraic equation

$$\chi^2\bar{n}_{es}^3 - 2\chi\Delta\bar{n}_{es}^2 + \bar{n}_{es}|\Gamma|^2 - \lambda^2 = 0 \quad (5)$$

that allows at most three real positive roots. A stable $\bar{n}_{es}$ must conform to the Hurwitz criterion (given by $\partial(\lambda^2)/\partial\bar{n}_{es} = 3\chi^2\bar{n}_{es}^2 - 4\bar{n}_{es}\chi\Delta + |\Gamma|^2 > 0$ here), which ensures that the system returns to the stable branch soon after the small perturbation. Therefore, if the conditions $|\Delta| > \sqrt{3}\gamma/2$ and $\Delta\chi > 0$ are satisfied, the bistable region will be given by $\bar{n}_{es} > \bar{n}_{es}^{(+)}$ or $\bar{n}_{es} < \bar{n}_{es}^{(-)}$ with the real positive $\bar{n}_{es}^{(\pm)} = (2\Delta \pm \sqrt{\Delta^2 - \frac{3}{4}\gamma^2})/3\chi$. For our interest, the dependence of $\bar{n}_{es}$ on the laser detuning Δ for a repulsive interatomic interaction ($\chi > 0$) is shown in Fig. 2(b), which exhibits optical bistability with hysteresis [43]. The coexistence of a low and a high Rydberg population in the off-resonance regime ($\Delta > 0$) leads to the bimodal counting distributions of the Rydberg excitation in experiment [46]. While for $\Delta = 0$, the bimodality can not arise due to the impossible bistability.

Linearized dynamics - The dissipative quantum dynamics for the system can be described by the master equation or the corresponding Fokker-Planck equation

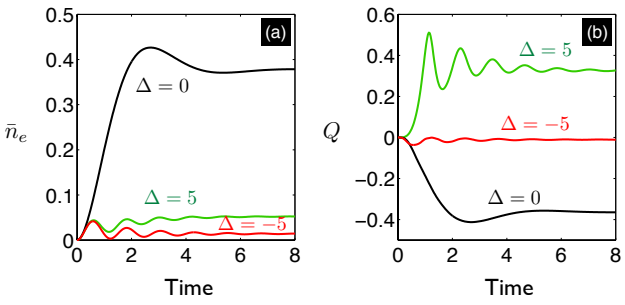

Figure 1. (a) Mean Rydberg population $\bar{n}_e$ and (b) Mandel Q parameter as a function of time for laser detunings $\Delta = -5$, 0 and 5 respectively. We fix units of $\gamma = 1$, taking $\lambda = 0.6$, $\chi = 10$. In all cases the population of the double-excitation state is less than 0.01. For $\Delta = 5$, the Rydberg excitation exhibits super-Poissonian counting statistics with $Q > 0$, while for $\Delta = -5$ and $\Delta = 0$, the sub-Poissonian processes characterized by $Q < 0$ are found.

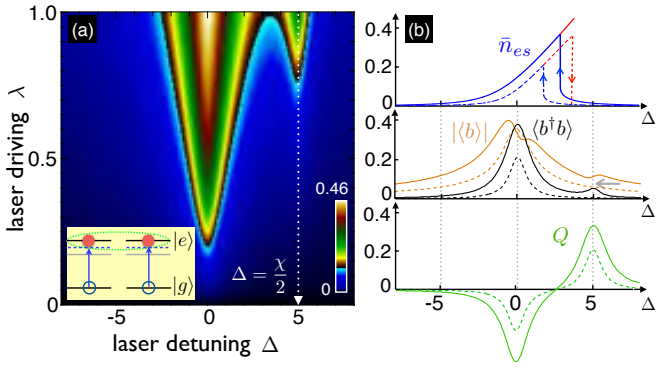

Figure 2. (a) Mean number of Rydberg excitations $\langle b^\dagger b\rangle$ in the steady state with full quantum theory as a function of λ and Δ. The inset shows the pair excitation of two atoms for $\Delta = \chi/2$. (b) Classical stationary mean $\bar{n}_{es}$, quantum mechanical steady-state solution of $\langle b^\dagger b\rangle$ and $|\langle b\rangle|$, and Mandel Q parameter versus laser detuning Δ with $\lambda = 0.3$ (dash) and $\lambda = 0.6$ (solid). Further parameters as in Fig. 1.

(FPE) [50]

$$\dot{P}(\alpha,\beta,t) = i[\frac{\partial}{\partial\alpha}(\Gamma\alpha + \chi\alpha^2\beta + \lambda) - \frac{\chi}{2}\frac{\partial^2}{\partial\alpha^2}\alpha^2 - \frac{\partial}{\partial\beta}(\Gamma^*\beta + \chi\beta^2\alpha + \lambda) + \frac{\chi}{2}\frac{\partial^2}{\partial\beta^2}\beta^2]P(\alpha,\beta,t) \tag{6}$$

by introducing the non-diagonal generalized P representation defined by

$$\rho(t) = \int_D d\sigma(\alpha,\beta)P(\alpha,\beta,t)\frac{|\alpha\rangle\langle\beta^*|}{\langle\beta^*|\alpha\rangle}, \tag{7}$$

where D is the integration domain, and $d\sigma$ is the integration measure that can be a volume integral $d^2\alpha d^2\beta$ over a complex phase space or a line integral $d\alpha d\beta$ over a manifold embedded in a complex phase space [50]. Note that α, β are arguments of the generalized P function (in correspondence to the c numbers of b, $b^\dagger$) and are complex conjugate in the mean $\bar{\alpha} = \bar{\beta}^*$.

Transforming the FPE into the Ito form yields a pair of stochastic differential equations (SDEs):

$$\frac{\partial}{\partial t}\begin{bmatrix}\alpha\\ \beta\end{bmatrix} = \begin{bmatrix}-i(\Gamma\alpha + \chi\alpha^2\beta + \lambda)\\ i(\Gamma^*\beta + \chi\beta^2\alpha + \lambda)\end{bmatrix} + \begin{bmatrix}-i\chi\alpha^2 & 0\\ 0 & i\chi\beta^2\end{bmatrix}^{\frac{1}{2}}\begin{bmatrix}\xi_1(t)\\ \xi_2(t)\end{bmatrix} \tag{8}$$

with $\xi_{1,2}(t)$ the delta-correlated Gaussian white noise, satisfying $\langle\xi_{1,2}(t)\rangle = 0$ and $\langle\xi_{1,2}(t)\xi_{1,2}(t')\rangle \sim \delta(t-t')$. We then linearize the SDEs around the classically steady-state solution $\bar{\alpha}_s(\bar{\beta}_s = \bar{\alpha}_s^*)$, and find that the quantum fluctuation $\delta\hat{\mathbf{X}} = [\delta\hat{\alpha}, \delta\hat{\beta}]^T$ close to the classical stable branches obeys the equation

$$\delta\dot{\hat{\mathbf{X}}} = -\boldsymbol{\mu}(\bar{\alpha}_s)\cdot\delta\hat{\mathbf{X}} + \mathbf{D}^{1/2}(\bar{\alpha}_s)\cdot\boldsymbol{\xi}(t), \tag{9}$$

where

$$\boldsymbol{\mu}(\bar{\alpha}_s) = -i\begin{bmatrix}\Gamma + 2\chi|\bar{\alpha}_s|^2 & -\chi\bar{\alpha}_s^{*2}\\ \chi\bar{\alpha}_s^2 & -\Gamma - 2\chi|\bar{\alpha}_s|^2\end{bmatrix} \tag{10}$$

and

$$\mathbf{D}(\bar{\alpha}_s) = \begin{bmatrix}-i\chi\bar{\alpha}_s^2 & 0\\ 0 & i\chi\bar{\alpha}_s^{*2}\end{bmatrix} \tag{11}$$

are the linearized drift and the diffusion array, respectively. The correlation matrix with regard to $\delta\hat{\mathbf{X}}$ can now be calculated through

$$\mathbf{C} = \begin{bmatrix}\langle b^2\rangle - \langle b\rangle^2 & \langle b^\dagger b\rangle - |\langle b\rangle|^2\\ \langle b^\dagger b\rangle - |\langle b\rangle|^2 & \langle b^{\dagger 2}\rangle - \langle b^\dagger\rangle^2\end{bmatrix} = \frac{\mathbf{D}\cdot\mathrm{Det}(\boldsymbol{\mu}) + [\boldsymbol{\mu}\mathbf{-I}\cdot\mathrm{Tr}(\boldsymbol{\mu})]\mathbf{D}[\boldsymbol{\mu}\mathbf{-I}\cdot\mathrm{Tr}(\boldsymbol{\mu})]^T}{2\mathrm{Tr}(\boldsymbol{\mu})\mathrm{Det}(\boldsymbol{\mu})} \tag{12}$$

The above result allows us to obtain the mean Rydberg population and the Mandel Q parameter in the linearized regime: [54]

$$\bar{n}_e \approx |\bar{\alpha}_s|^2 + \langle\delta\hat{\alpha}^\dagger\delta\hat{\alpha}\rangle = \bar{n}_{es} + \frac{\chi^2}{2\Lambda}\bar{n}_{es}^2, \tag{13}$$

$$Q \approx 2\bar{n}_{es}\mathrm{Re}[\langle\delta\hat{\alpha}^2\rangle/\bar{\alpha}_s^2] + 2\langle\delta\hat{\alpha}^\dagger\delta\hat{\alpha}\rangle = \frac{\bar{n}_{es}\chi}{\Lambda}(\Delta - \chi\bar{n}_{es}), \tag{14}$$

with $\Lambda = |\Gamma|^2 - 4\chi\Delta\bar{n}_{es} + 3\chi^2\bar{n}_{es}^2$. The steady-state solution $\bar{n}_{es}$ can be obtained by solving the set of classically nonlinear equations (4), and there may exist two stable solution for a well-selected laser detuning as shown in Fig.2(b). We now assume this solution has been found and focus on the effect of the quantum fluctuations. One of the intriguing effects can be found in the asymptotic expansion of $\bar{n}_e$ to the first-order [see Eq. (13)], where the Rydberg population is enhanced by the Rydberg-Rydberg coupling via the intensity of quantum fluctuation $\langle\delta\hat{\alpha}^\dagger\delta\hat{\alpha}\rangle$ [34, 37]. Second, due to the Rydberg-Rydberg interactions, the laser field drives the atomic transition from the ground state to the Rydberg state in a cooperative manner, with the fluctuations of the collective excitation number being characterized by the Mandel Q factor. The results show that the collective excitation number exhibits super-Poissonian distribution for the laser detuning Δ greater than the collective energy shift $\bar{n}_{es}\chi$ ($\Delta/\bar{n}_{es}\chi > 1$) and sub-Poissonian distribution for the other ($\Delta/\bar{n}_{es}\chi < 1$), leading to collective quantum jumps while the system stays in the two classically stable branches [34]. The linear theory breaks down for $\Lambda \to 0$ (corresponding to the violation of the Hurwitz criterion), in which case $\bar{n}_{es}$ approaches the onset of instability.

Full quantum dynamics - Having seen the effect of the quantum fluctuations based on the linearization, we next address the question with full quantum theory. In the quantum noise limit, there exists an exact steady-state

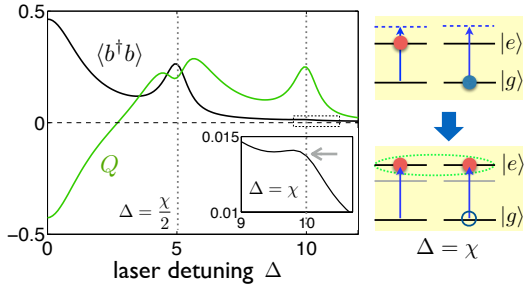

Figure 3. Left panel: Quantum mechanical steady-state solution of mean Rydberg population $\langle b^\dagger b\rangle$ and Mandel Q parameter versus laser detuning Δ with increasing driving strength $\lambda = 1$ and $\chi = 10$. Right panel: An already excited Rydberg atom forwards the excitation of the surrounding atoms interacting with it for $\Delta = \chi$. See the text for detail.

solution $P_{ss}(\alpha,\beta) = \alpha^{c-2}\beta^{d-2}exp[-z(1/\alpha + 1/\beta) + 2\alpha\beta$ for the FPE (6) with $z = 2\lambda/\chi$, $c = 2\Gamma/\chi$, and $d = c^*$ [54]. While we obtain the generalized P function, the Rydberg population and the Rydberg counting statistics can be calculated via

$$\langle b^{\dagger n} b^m\rangle = \frac{\int_D d\sigma(\alpha,\beta)P_{ss}(\alpha,\beta)\beta^n\alpha^m}{\int_D d\sigma(\alpha,\beta)P_{ss}(\alpha,\beta)}. \tag{15}$$

The appropriate integration domain D here will be a complex manifold embedded in the space $\mathbb{C}^2$ and each path of integration is chosen to be a Hankel path $\mathcal{O}$. These ensure that the distribution function $P(\alpha,\beta)$ vanishes correctly at the boundary. Skipping over the fussy calculations we finally come at [54]

$$\langle b\rangle = \frac{z}{c}\frac{{}_0F_2(c+1,d,2z^2)}{{}_0F_2(c,d,2z^2)}, \tag{16}$$

$$\langle b^\dagger b\rangle = \frac{z^2}{cd}\frac{{}_0F_2(c+1,d+1,2z^2)}{{}_0F_2(c,d,2z^2)}, \tag{17}$$

$$Q = \frac{z^2}{(c+1)(d+1)}\frac{{}_0F_2(c+2,d+2,2z^2)}{{}_0F_2(c+1,d+1,2z^2)} - \frac{z^2}{cd}\frac{{}_0F_2(c+1,d+1,2z^2)}{{}_0F_2(c,d,2z^2)}, \tag{18}$$

where ${}_0F_2(c,d,z)$ is a hypergeometric series defined as

$${}_0F_2(c,d,z) = \sum_{n=0}^{\infty}\frac{z^n}{n!}\frac{\Gamma(c)\Gamma(d)}{\Gamma(c+n)\Gamma(d+n)} \tag{19}$$

with $\Gamma(x) = [\frac{z^{1-x}}{2\pi i}\int_{\mathcal{O}}\sigma^{-x}e^{\sigma z}d\sigma]^{-1}$ the gamma-function.

The phase diagram for the mean number of Rydberg excitations in (λ,Δ) space shows that the Rydberg excitation dramatically increases at the laser detunings $\Delta = 0$ and $\Delta = \chi/2$ [see Fig. 2(a)], which corresponds to individually resonant excitation of the each atom and pair excitation of the interacting atoms, respectively. Numerical simulation proves that the system is confined in the subspace spanned by the null- and double-excitation states for $\Delta = \chi/2$ without considering the relaxation, confirming that for this detuning the atomic excitation is caused by the two-photon process; this is fundamentally different from the case of resonant driving, where the system has no probability of being pumped to the state with more than one excitation due to the Rydberg blockade. The excitation processes exhibit the sub-Poissonian character on resonance and super-Poissonian character for the other. For $0 < \Delta < \chi/2$, both the individual excitation and the pair excitation are possible. While the classical dynamics predicts an optical bistability, the quantum mechanical calculation including the interatomic correlation does not exhibit bistability. It should also be noted that the pair excitation of two atoms is a pure quantum effect that is unable to be revealed by the classical theory [see arrow in Fig. 2(b)] [54]. An extra quantum signature for the system is given by the dips in the laser-detuning dependence of $|\langle b\rangle|$, which arise because of the out-of-phase quantum fluctuations between the two classical branches. This is the evidence for the quantum-fluctuation driven two-state transitions [34] that results in the bimodal counting distribution of the Rydberg population and strongly relates to the nonequilibrium first-order dynamical phase transition [16, 32].

Increasing the laser intensity will enhance the mean number of Rydberg excitations for $\Delta = \chi/2$, but meanwhile weaken the super-Poissonian excitation process due to the decreasing ratio $\Delta/\bar{n}_{es}\chi$, as shown in Fig. 3. This fact can be directly understood from the linearized calculation Eq. (14)]. For the far off-resonance regime $\Delta \gg \Omega$, there is a small chance (roughly $\Omega^2/4\Delta$) for an atom being excited to the Rydberg state if all the atoms are initially in the ground state. However, while an atom has been luckily excited by the laser beam with the detuning $\Delta = \chi$, then similar to the Rydberg aggregates, the surrounding atoms tend to be excited cooperatively due to the Rydberg-Rydberg coupling, as sketched in the right panel of Fig. 3.

Conclusion - We have analyzed the steady-state excitation dynamics of a weakly-driven Rydberg-atom system by treating the inhomogeneous Rydberg-Rydberg interaction as a all-to-all coupling, for which the experimentally accessible parameter regime is described in ref. [34]. The analytical calculation allows us to find the effect of the quantum fluctuations on the Rydberg excitation process and the quantum phenomena such as simultaneous bi-excitation of Rydberg atoms and interaction-assisted Rydberg excitation, which are referred to as the quantum signature of the system. The simplified picture will be significant for quantitatively understanding the Rydberg aggregates [44, 45], bimodal counting distribution [46], and kinetic constraints [47] in recent experimental observations with Rydberg atoms, and more generally

the many-body effect for the interacting spin-1/2 systems [51].

This work was supported by the Major State Basic Research Development Program of China under Grant No. 2012CB921601; the National Natural Science Foundation of China under Grants Nos. 11305037, 11347114, 11374054 and 11422437; the Natural Science Foundation of Fujian Province under Grant No. 2013J01012.

[1] M. Saffman, T. G. Walker, and K. Mølmer, Rev. Mod. Phys. **82**, 2313 (2010).
[2] D. E. Chang, V. Vuletić, and M. D. Lukin, Nat. Photon. **8**, 685 (2014).
[3] J. D. Pritchard, D. Maxwell, A. Gauguet, K. J. Weatherill, M. P. A. Jones, and C. S. Adams, Phys. Rev. Lett. **105**, 193603 (2010).
[4] S. Sevinçli, N. Henkel, C. Ates, and T. Pohl, Phys. Rev. Lett. **107**, 153001 (2011).
[5] D. Petrosyan, J. Otterbach, and M. Fleischhauer, Phys. Rev. Lett. **107**, 213601 (2011).
[6] T. Peyronel, O. Firstenberg, Q.-Y. Liang, S. Hofferberth, A. V. Gorshkov, T. Pohl, M. D. Lukin, and V. Vuletić, Nature (London) **488**, 57 (2012).
[7] V. Parigi, E. Bimbard, J. Stanojevic, A. J. Hilliard, F. Nogrette, R. Tualle-Brouri, A. Ourjoumtsev, and P. Grangier, Phys. Rev. Lett. **109**, 233602 (2012).
[8] D. Yan, Y.-M. Liu, Q.-Q. Bao, C.-B. Fu, and J.-H. Wu, Phys. Rev. A **86**, 023828 (2012).
[9] A. V. Gorshkov, R. Nath, and T. Pohl, Phys. Rev. Lett. **110**, 153601 (2013).
[10] D. Maxwell, D. J. Szwer, D. Paredes-Barato, H. Busche, J. D. Pritchard, A. Gauguet, K. J. Weatherill, M. P. A. Jones, and C. S. Adams, Phys. Rev. Lett. **110**, 103001 (2013).
[11] B. He, A. V. Sharypov, J. Sheng, C. Simon, and M. Xiao, Phys. Rev. Lett. **112**, 133606 (2014).
[12] W. Li, D. Viscor, S. Hofferberth, and I. Lesanovsky, Phys. Rev. Lett. **112**, 243601 (2014).
[13] M. F. Maghrebi, M. J. Gullans, P. Bienias, S. Choi, I. Martin, O. Firstenberg, M. D. Lukin, H. P. Büchler, and a. V. Gorshkov, Phys. Rev. Lett **115**, 123601 (2015).
[14] H. Weimer, R. Löw, T. Pfau, and H. P. Büchler, Phys. Rev. Lett. **101**, 250601 (2008).
[15] H. Weimer and H. P. Büchler, Phys. Rev. Lett. **105**, 230403 (2010).
[16] T. E. Lee, H. Häffner, and M. C. Cross, Phys. Rev. A **84**, 031402 (2011).
[17] J. Qian, G. Dong, L. Zhou, and W. Zhang, Phys. Rev. A **85**, 065401 (2012).
[18] I. Lesanovsky and J. P. Garrahan, Phys. Rev. Lett. **111**, 215305 (2013).
[19] M. Marcuzzi, E. Levi, S. Diehl, J. P. Garrahan, and I. Lesanovsky, Phys. Rev. Lett. **113**, 210401 (2014).
[20] M. Hoening, W. Abdussalam, M. Fleischhauer, and T. Pohl, Phys. Rev. A **90**, 021603 (2014).
[21] A. W. Glaetzle, R. Nath, B. Zhao, G. Pupillo, and P. Zoller, Phys. Rev. A **86**, 043403 (2012).
[22] M. Höning, D. Muth, D. Petrosyan, and M. Fleischhauer, Phys. Rev. A **87**, 023401 (2013).
[23] B. Vermersch, M. Punk, A. W. Glaetzle, C. Gross, and P. Zoller, New J. Phys. **17**, 013008 (2015).
[24] C. Ates, T. Pohl, T. Pattard, and J. M. Rost, Phys. Rev. Lett. **98**, 023002 (2007).
[25] C. Ates, T. Pohl, T. Pattard, and J. Rost, Phys. Rev. A **76**, 013413 (2007).
[26] M. Mayle, W. Zeller, N. Tezak, and P. Schmelcher, Phys. Rev. A **84**, 010701 (2011).
[27] C. Ates and I. Lesanovsky, Phys. Rev. A **86**, 013408 (2012).
[28] D. Petrosyan, M. Höning, and M. Fleischhauer, Phys. Rev. A **87**, 053414 (2013).
[29] M. Gärttner, K. P. Heeg, T. Gasenzer, and J. Evers, Phys. Rev. A **88**, 043410 (2013).
[30] S. Bettelli, D. Maxwell, T. Fernholz, C. S. Adams, I. Lesanovsky, and C. Ates, Phys. Rev. A **88**, 043436 (2013).
[31] J. Sanders, M. Jonckheere, and S. Kokkelmans, Phys. Rev. Lett. **115**, 043002 (2015).
[32] C. Ates, B. Olmos, J. P. Garrahan, and I. Lesanovsky, Phys. Rev. A **85**, 043620 (2012).
[33] T. E. Lee and M. C. Cross, Phys. Rev. A **85**, 063822 (2012).
[34] T. E. Lee, H. Häffner, and M. C. Cross, Phys. Rev. Lett. **108**, 023602 (2012).
[35] A. Hu, T. E. Lee, and C. W. Clark, Phys. Rev. A **88**, 053627 (2013).
[36] D. W. Schönleber, M. Gärttner, and J. Evers, Phys. Rev. A **89**, 033421 (2014).
[37] M. Gärttner, S. Whitlock, D. W. Schönleber, and J. Evers, Phys. Rev. Lett. **113**, 233002 (2014).
[38] B. Olmos, D. Yu, and I. Lesanovsky, Phys. Rev. A **89**, 023616 (2014).
[39] H. Weimer, Phys. Rev. A **91**, 063401 (2015).
[40] H. Schempp, G. Günter, S. Wüster, M. Weidemüller, and S. Whitlock, Phys. Rev. Lett. **115**, 093002 (2015).
[41] M. Viteau, P. Huillery, M. G. Bason, N. Malossi, D. Ciampini, O. Morsch, E. Arimondo, D. Comparat, and P. Pillet, Phys. Rev. Lett. **109**, 053002 (2012).
[42] C. S. Hofmann, G. Günter, H. Schempp, M. Robert-de Saint-Vincent, M. Gärttner, J. Evers, S. Whitlock, and M. Weidemüller, Phys. Rev. Lett. **110**, 203601 (2013).
[43] C. Carr, R. Ritter, C. G. Wade, C. S. Adams, and K. J. Weatherill, Phys. Rev. Lett. **111**, 113901 (2013).
[44] H. Schempp, G. Günter, M. Robert-de Saint-Vincent, C. S. Hofmann, D. Breyel, A. Komnik, D. W. Schönleber, M. Gärttner, J. Evers, S. Whitlock, et al., Phys. Rev. Lett. **112**, 013002 (2014).
[45] A. Urvoy, F. Ripka, I. Lesanovsky, D. Booth, J. P. Shaffer, T. Pfau, and R. Löw, Phys. Rev. Lett. **114**, 203002 (2015).
[46] N. Malossi, M. M. Valado, S. Scotto, P. Huillery, P. Pillet, D. Ciampini, E. Arimondo, and O. Morsch, Phys. Rev. Lett. **113**, 023006 (2014).
[47] M. M. Valado, C. Simonelli, M. D. Hoogerland, I. Lesanovsky, J. P. Garrahan, E. Arimondo, D. Ciampini, O. Morsch, and F. E. Fermi, arXiv:1508.04384v2.
[48] G. Günter, M. Robert-de Saint-Vincent, H. Schempp, C. S. Hofmann, S. Whitlock, and M. Weidemüller, Phys. Rev. Lett. **108**, 013002 (2012).
[49] A. Schwarzkopf, R. E. Sapiro, and G. Raithel, Phys. Rev. Lett. **107**, 103001 (2011).
[50] P. D. Drummond and D. F. Walls, Journal of Physics A:

Mathematical and General **13**, 725 (1980).
[51] J. W. Britton, B. C. Sawyer, A. C. Keith, C. C. J. Wang, J. K. Freericks, H. Uys, M. J. Biercuk, and J. J. Bollinger, Nature (London) **484**, 489 (2012).
[52] C. P. Sun, Y. Li, and X. F. Liu, Phys. Rev. Lett. **91**, 147903 (2003).
[53] K. Hammerer, A. S. Sørensen, and E. S. Polzik, Rev. Mod. Phys. **82**, 1041 (2010).
[54] See supplemental material.

arXiv:1512.00696v1 [quant-ph] 2 Dec 2015

Supplemental Material

In this supplemental material, we will show that the exact simulation of the Hamiltonian H in the main text with spin operators for few atoms is found to be in good agreement with the theoretical model in terms of bosonic operators. We also show how to obtain the correlation matrix under linearization and the analytical steady-state solution for the Fokker-Planck equation as in ref. [1] discussing the optical bistability for nonlinear polarisability model. The nonclassical nature of the quantum mechanical steady states is also shown by the Wigner functions.

1 The exact simulation of the dissipative dynamics with atomic spin operators

The exactly dissipative dynamics of the laser-driven system with the Hamiltonian H in the main text can be described by the master equation

$$\dot{\rho} = \frac{1}{i\hbar}[H, \rho] + \frac{\gamma}{2}\sum_{j=1}^{N}\mathcal{L}_j, \tag{1}$$

where

$$\mathcal{L}_j = 2\sigma_{ge}^{(j)}\rho\sigma_{eg}^{(j)} - \sigma_{eg}^{(j)}\sigma_{ge}^{(j)}\rho - \rho\sigma_{eg}^{(j)}\sigma_{ge}^{(j)}, \tag{2}$$

$\sigma_{ge}^{(j)} = |g_j\rangle\langle e_j|$ and $\sigma_{eg}^{(j)} = |e_j\rangle\langle g_j|$. With the excitation-number operator being $\hat{n}_e = \sum_{j=1}^{N}|e_j\rangle\langle e_j|$, the mean number of Rydberg excitations and the Mandel Q parameter can be calculated via $\bar{n}_e = \mathrm{Tr}(\rho\hat{n}_e)$ and $Q = \mathrm{Tr}(\rho(\Delta\hat{n}_e)^2)/\mathrm{Tr}(\rho\hat{n}_e) - 1$, respectively.

Simulating the Eq. (1) with $N = 6$, we show the time-dependent mean Rydberg population $\bar{n}_e$ and Mandel Q parameter in Fig. 1, and the steady-state solution of $\bar{n}_e$ and Q versus laser detuning Δ in Fig. 2, which demonstrate the quantitatively good agreement with the results obtained via the simulation of the bosonization model.

2 The quantum fluctuation under linearization

Splitting the operators b ($b^\dagger$) into classical and quantum parts $\alpha = \bar{\alpha} + \delta\hat{\alpha}(t)$, $\beta = \bar{\beta} + \delta\hat{\beta}(t)$ ($\bar{\alpha}^* = \bar{\beta}$), we obtain the linearized correlation matrix given by

$$\mathbf{C} = \begin{bmatrix} \langle b^2\rangle - \langle b\rangle^2 & \langle b^\dagger b\rangle - |\langle b\rangle|^2 \\ \langle b^\dagger b\rangle - |\langle b\rangle|^2 & \langle b^{\dagger 2}\rangle - \langle b^\dagger\rangle^2 \end{bmatrix}$$

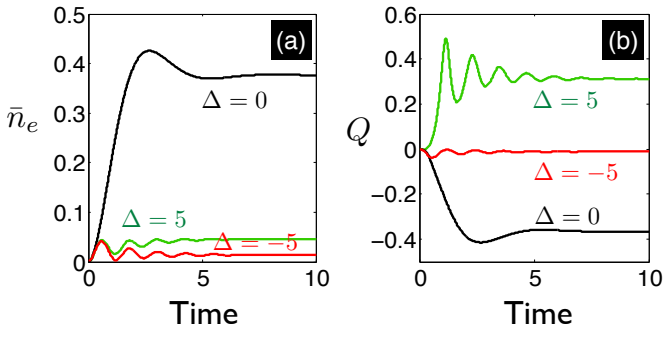

Figure 1: (a) Mean Rydberg population $\bar{n}_e$ and (b) Mandel Q parameter as a function of time for laser detunings $\Delta = -5$, 0 and 5 respectively. Further parameters as in Fig. 1 in the main text.

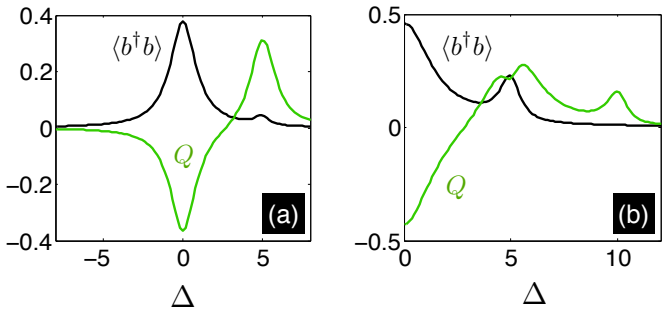

Figure 2: Quantum mechanical steady-state solution of $\bar{n}_e$ and Mandel Q parameter versus laser detuning Δ for (a) $\lambda = 0.6$ and (b) $\lambda = 1$. Further parameters as in Fig. 2(b) in the main text.

$$= \begin{bmatrix} \langle \delta\hat{\alpha}^2 \rangle & \langle \delta\hat{\alpha}^\dagger \delta\hat{\alpha} \rangle \\ \langle \delta\hat{\alpha}^\dagger \delta\hat{\alpha} \rangle & \langle \delta\hat{\alpha}^{\dagger 2} \rangle \end{bmatrix} \tag{3}$$

where

$$\langle \delta\hat{\alpha}^2 \rangle = -\frac{\chi\bar{\alpha}^2(\Gamma^* + 2\chi\bar{n}_{es})}{2\Lambda}, \tag{4}$$

$$\langle \delta\hat{\alpha}^\dagger \delta\hat{\alpha} \rangle = \frac{\chi^2\bar{n}_{es}^2}{2\Lambda} \tag{5}$$

and

$$\langle \delta\hat{\alpha}^{\dagger 2} \rangle = -\frac{\chi\bar{\alpha}^{*2}(\Gamma + 2\chi\bar{n}_{es})}{2\Lambda} \tag{6}$$

with $\Lambda = \frac{\gamma^2}{4} + \Delta^2 - 4\chi\Delta\bar{n}_{es} + 3\chi^2\bar{n}_{es}^2$ are obtained from $\mathbf{C} = \frac{\mathbf{D}\cdot\mathrm{Det}(\boldsymbol{\mu}) + [\boldsymbol{\mu} - \mathbf{I}\cdot\mathrm{Tr}(\boldsymbol{\mu})]\mathbf{D}[\boldsymbol{\mu} - \mathbf{I}\cdot\mathrm{Tr}(\boldsymbol{\mu})]^T}{2\mathrm{Tr}(\boldsymbol{\mu})\mathrm{Det}(\boldsymbol{\mu})}$ by using the drift and diffusion arrays. Thus, the mean number of Rydberg excitations and the Mandel Q parameter, in the linearized regime, are given by

$$\bar{n}_e \approx |\bar{\alpha}|^2 + \langle \delta\hat{\alpha}^\dagger \delta\hat{\alpha} \rangle = \bar{n}_{es} + \frac{\chi^2}{2\Lambda}\bar{n}_{es}^2 \tag{7}$$

and

$$\begin{aligned} Q &= \frac{[\langle (b^\dagger b)^2 \rangle - \langle b^\dagger b \rangle^2]}{\langle b^\dagger b \rangle} - 1 \\ &= \frac{2\mathrm{Re}[\bar{\alpha}^{*2}\langle \delta\hat{\alpha}^2 \rangle] + 2\bar{n}_{es}\langle \delta\hat{\alpha}^\dagger \delta\hat{\alpha} \rangle}{\bar{n}_{es} + \langle \delta\hat{\alpha}^\dagger \delta\hat{\alpha} \rangle} + O[(\delta\hat{\alpha}^\dagger)^2(\delta\hat{\alpha})^2], \end{aligned} \tag{8}$$

respectively. For $\langle \delta\hat{\alpha}^\dagger \delta\hat{\alpha} \rangle \ll \bar{n}_{es}$, and keeping only the first-order fluctuation, the Mandel Q parameter approximates to

$$\begin{aligned} Q &\approx 2\mathrm{Re}[\langle \delta\hat{\alpha}^2 \rangle / \bar{\alpha}^2] + 2\langle \delta\hat{\alpha}^\dagger \delta\hat{\alpha} \rangle \\ &= \frac{\bar{n}_{es}\chi}{\Lambda}(\Delta - \chi\bar{n}_{es}). \end{aligned} \tag{9}$$

It should be realized that the mean Rydberg population is enhanced by the intensity of quantum fluctuation $\langle \delta\hat{\alpha}^\dagger \delta\hat{\alpha} \rangle$ induced by the Rydberg-Rydberg interaction. Moreover, the Mandel Q parameter is additionally affected by the quantum fluctuation $\langle \delta\hat{\alpha}^2 \rangle$ around $\langle b \rangle$. The cooperation of the quantum fluctuations $\langle \delta\hat{\alpha}^2 \rangle$ and $\langle \delta\hat{\alpha}^\dagger \delta\hat{\alpha} \rangle$ finally determines the statistical dynamics of the Rydberg excitation, in correspondence to the super(sub)-Poissonian counting statistics. On the other hand, the Hurwitz criteria for stability is given by $\Lambda > 0$. While Λ approaches to zero, the quantum fluctuations diverges and the linearization fails.

3 The exact solution of the Fokker-Planck equation

Consider the Fokker-Planck equation (in the quantum noise limit, excluding the thermal noise, i.e. $n_{th} = 0$)

$$\begin{aligned} \dot{P}(\alpha,\beta,t) &= [\partial_u \mathbf{A}_u(\alpha,\beta) + \frac{1}{2}\partial_u\partial_v \mathbf{D}_{uv}(\alpha,\beta)]P(\alpha,\beta,t) \\ &= \partial_u\{\frac{1}{2}\mathbf{D}_{uv}[(\mathbf{D}_{vu})^{-1}(2\mathbf{A}_u + \partial_v \mathbf{D}_{uv})P + \partial_v P\} \end{aligned} \tag{10}$$

with $u, v = \alpha, \beta$, and the diffusion array is

$$\mathbf{D}(\alpha,\beta) = \begin{bmatrix} -i\chi\alpha^2 & 0 \\ 0 & i\chi\beta^2 \end{bmatrix}, \tag{11}$$

$$\mathbf{A}(\alpha,\beta) = \begin{bmatrix} i(\Gamma\alpha + \chi\alpha^2\beta + \lambda) \\ -i(\Gamma^*\beta + \chi\beta^2\alpha + \lambda) \end{bmatrix}. \tag{12}$$

A steady-state exact solution for the Fokker-Planck equation exists only when the conditional equations $\partial_u V_v = \partial_v V_u$ are fulfilled [2], where the potential function is given by $V_\varrho = (\mathbf{D}_{\varrho u})^{-1}(2\mathbf{A}_u + \partial_\sigma \mathbf{D}_{u\sigma})$, $\varrho = 1, 2$, that is

$$\begin{bmatrix} V_1 \\ V_2 \end{bmatrix} = -\frac{2}{\chi}\begin{bmatrix} (\Gamma - \chi)/\alpha + \chi\beta + \lambda/\alpha^2 \\ (\Gamma^* - \chi)/\beta + \chi\alpha + \lambda/\beta^2 \end{bmatrix}. \tag{13}$$

It is straightforward to verified that $\partial_\beta V_1 = \partial_\alpha V_2 = -2$ here. Thus, in the stationary limit $\dot{P}(\alpha,\beta,t=\infty) = 0$, we have

$$[\partial_u \mathbf{A}_u(\alpha,\beta) + \frac{1}{2}\partial_u\partial_v \mathbf{D}_{uv}(\alpha,\beta)]P(\alpha,\beta,t) = 0 \tag{14}$$

or

$$\partial_u\{\mathbf{D}_{uv}[(\mathbf{D}_{vu})^{-1}(2\mathbf{A}_u + \partial_v \mathbf{D}_{uv})P + \partial_v P\} = 0. \tag{15}$$

The exact solution for the Fokker-Planck equation is therefore given by

$$\begin{aligned} P_{ss}(\alpha,\beta) &= exp(-\int^{(\mathbb{C}_\alpha,\mathbb{C}_\beta)_\varrho} \mathbf{V}_\varrho(\alpha,\beta)d(\alpha,\beta)_\varrho) \\ &= exp\{\frac{2}{\chi}\int^{\mathbb{C}_\alpha}[(\Gamma-\chi)/\alpha + \chi\beta + \lambda/\alpha^2]d\alpha \\ &\quad + \frac{2}{\chi}\int^{\mathbb{C}_\beta}[(\Gamma^*-\chi)/\beta + \chi\alpha + \lambda/\beta^2]d\beta\} \\ &= exp\{\frac{2}{\chi}[(\Gamma-\chi)ln\alpha - \lambda/\alpha] + \frac{2}{\chi}[(\Gamma^*-\chi)ln\beta - \lambda/\beta] \\ &\quad + 2\int^{(\mathbb{C}_\alpha,\mathbb{C}_\beta)}(\alpha d\beta + \beta d\alpha)\} \\ &= \alpha^{c-2}\beta^{d-2}exp[-z(1/\alpha + 1/\beta) + 2\alpha\beta], \end{aligned} \tag{16}$$

where $z = 2\lambda/\chi$ and $c = 2\Gamma/\chi$ ($d = c^*$) are dimensionless quantities. Note that no Glauber-Sudarshan $P(\alpha,\alpha^*)$ function exists in the steady state with $\beta = \alpha^*$ due to the diverging exponential factor $\exp(2\alpha\alpha^*)$, except as a generalized form $P(\alpha,\beta)$.

The generalized $P(\alpha,\beta)$ function has to satisfying the normalization condition, which implies

$$\begin{aligned} I &= \int^{(\mathbb{C}_\alpha,\mathbb{C}_\beta)} P_{ss}(\alpha,\beta)d\alpha d\beta \\ &= \int^{(\mathbb{C}_\alpha,\mathbb{C}_\beta)} d\alpha d\beta \alpha^{c-2}\beta^{d-2}e^{-z(1/\alpha+1/\beta)+2\alpha\beta} \\ &= \int^{(\mathbb{C}_\alpha,\mathbb{C}_\beta)} d(\alpha^{-1})d(\beta^{-1})\sum_{n=0}^{\infty}\frac{2^n}{n!}\alpha^{c+n}\beta^{d+n}e^{-z(1/\alpha+1/\beta)} \\ &= \int^{(\mathbb{C}_\alpha,\mathbb{C}_\beta)} d\alpha_1 d\beta_1 \sum_{n=0}^{\infty}\frac{2^n}{n!}\alpha_1^{-(c+n)}\beta_1^{-(d+n)}e^{-z(\alpha_1+\beta_1)} \end{aligned} \tag{17}$$

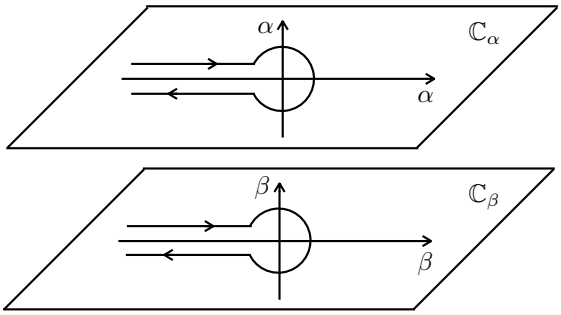

Figure 3: The Hankel path of integration.

with $\alpha_1 = \alpha^{-1}$ and $\beta_1 = \beta^{-1}$. On the other hand, the Gamma-function identity can be defined by using the Hankel path of integration $\mathcal{O}$ (see Fig. 3)

$$\begin{aligned}\frac{1}{\Gamma(c+n)} &= \frac{1}{2\pi i}\int_{\mathcal{O}}(\sigma z)^{-(c+n)}e^{\sigma z}d(\sigma z)\\ &= \frac{z^{1-(c+n)}}{2\pi i}\int_{\mathcal{O}}\sigma^{-(c+n)}e^{\sigma z}d\sigma,\end{aligned} \tag{18}$$

with which we obtain

$$\begin{aligned}I &= \int^{(\mathbb{C}_\alpha,\mathbb{C}_\beta)} d\alpha_1 d\beta_1 \sum_{n=0}^{\infty}\frac{2^n}{n!}\alpha_1^{-(c+n)}\beta_1^{-(d+n)}e^{-z(\alpha_1+\beta_1)}\\ &= \sum_{n=0}^{\infty}\frac{2^n}{n!}[\int_{\mathcal{O}}d\alpha_1\alpha_1^{-(c+n)}e^{-z\alpha_1}\int_{\mathcal{O}}d\beta_1\beta_1^{-(d+n)}e^{-z\beta_1}]\\ &= (-4\pi^2)\sum_{n=0}^{\infty}\frac{2^n}{n!}\frac{z^{c+d+2(n-1)}}{\Gamma(c+n)\Gamma(d+n)}\\ &= \frac{(-4\pi^2)z^{c+d-2}}{\Gamma(c)\Gamma(d)}{}_0F_2(c,d,2z^2),\end{aligned} \tag{19}$$

where ${}_0F_2(c,d,z)$ is the generalized hypergeometric function defined as

$${}_0F_2(c,d,z) = \sum_{n=0}^{\infty}\frac{z^n}{n!}\frac{\Gamma(c)\Gamma(d)}{\Gamma(c+n)\Gamma(d+n)}. \tag{20}$$

The normalized ith-order correlation function $G^{(i,j)}$ corresponding to the normally ordered averages $\langle b^{\dagger i}b^j\rangle$ can be calculated by the generalized P-representation:

$$\begin{aligned}G^{(i,j)} &= \frac{\int d\sigma(\alpha,\beta)P(\alpha,\beta)\beta^m\alpha^n}{\int d\sigma(\alpha,\beta)P(\alpha,\beta)}\\ &= \frac{\frac{(-4\pi^2)z^{c+d-2+i+j}}{\Gamma(c+j)\Gamma(d+i)}{}_0F_2(c+j,d+i,2z^2)}{\frac{(-4\pi^2)z^{c+d-2}}{\Gamma(c)\Gamma(d)}{}_0F_2(c,d,2z^2)}.\end{aligned} \tag{21}$$

With the Euler's functional equation $\Gamma(z)/\Gamma(z+n+1) = 1/z(z+1)\cdots(z+n)$, we finally have

$$G^{(i,j)} = z^{i+j}\frac{\Gamma(c)\Gamma(d){}_0F_2(c+j,d+i,2z^2)}{\Gamma(c+j)\Gamma(d+i){}_0F_2(c,d,2z^2)}, \tag{22}$$

and therefore the quantum mechanical steady-state solution of $\langle b\rangle$, $\langle b^\dagger b\rangle$ and $Q = \frac{\langle b^\dagger b^\dagger bb\rangle}{\langle b^\dagger b\rangle} - \langle b^\dagger b\rangle$.

4 The nonclassical nature of the quantum mechanical steady states

The nonclassical nature of the quantum mechanical steady states for the excitation processes with resonant driving and the laser detuning $\Delta = \chi/2$ manifests itself in the Wigner function with negative value, as shown in figure 4.

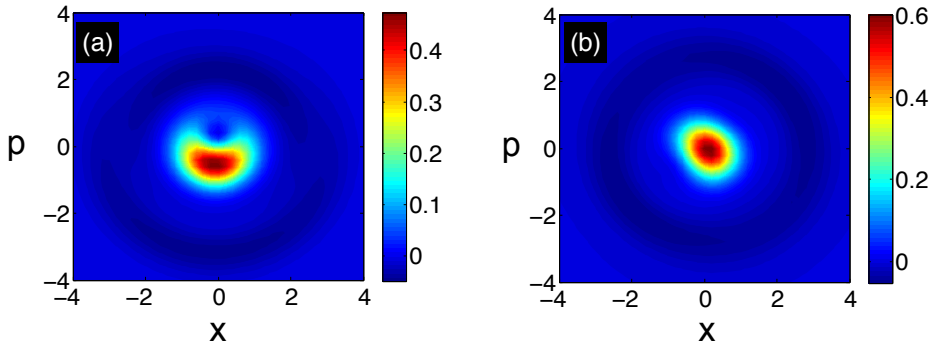

Figure 4: Wigner function $W(x, p)$ of the quantum mechanical steady-state solution with (a) $\Delta = 0$ and (b) $\Delta = \chi/2$.

References

[1] P. D. Drummond and D. F. Walls. Quantum theory of optical bistability. i. nonlinear polarisability model. *Journal of Physics A: Mathematical and General*, 13(2):725, 1980.

[2] H. Haken. Cooperative phenomena in systems far from thermal equilibrium and in nonphysical systems. *Rev. Mod. Phys.*, 47:67–121, Jan 1975.